



**HAL**  
open science

## Measurement of $^{230}\text{Pa}$ and $^{186}\text{Re}$ production cross sections induced by deuterons at Arronax facility

Charlotte Duchemin, Arnaud Guertin, Vincent Métivier, Ferid Haddad,  
Nathalie Michel

### ► To cite this version:

Charlotte Duchemin, Arnaud Guertin, Vincent Métivier, Ferid Haddad, Nathalie Michel. Measurement of  $^{230}\text{Pa}$  and  $^{186}\text{Re}$  production cross sections induced by deuterons at Arronax facility. CRETE13 : 2013 International Conference on Applications of Nuclear Techniques, Jun 2013, Rethymon, Crète, Greece. pp.1460149, 10.1142/S2010194514601495 . hal-01082278

**HAL Id: hal-01082278**

**<https://hal.science/hal-01082278>**

Submitted on 15 Jan 2021

**HAL** is a multi-disciplinary open access archive for the deposit and dissemination of scientific research documents, whether they are published or not. The documents may come from teaching and research institutions in France or abroad, or from public or private research centers.

L'archive ouverte pluridisciplinaire **HAL**, est destinée au dépôt et à la diffusion de documents scientifiques de niveau recherche, publiés ou non, émanant des établissements d'enseignement et de recherche français ou étrangers, des laboratoires publics ou privés.

## MEASUREMENT OF $^{230}\text{Pa}$ AND $^{186}\text{Re}$ PRODUCTION CROSS SECTIONS INDUCED BY DEUTERONS AT ARRONAX FACILITY

CHARLOTTE DUCHEMIN, ARNAUD GUERTIN, VINCENT METIVIER

*Laboratoire SUBATECH, Ecole des Mines de Nantes, Université de Nantes, CNRS/IN2P3  
4, rue Alfred Kastler, La Chantrerie  
Nantes, 44307, France  
Charlotte.Duchemin@subatech.in2p3.fr*

FERID HADDAD, NATHALIE MICHEL

*Laboratoire SUBATECH, Ecole des Mines de Nantes, Université de Nantes, CNRS/IN2P3  
4, rue Alfred Kastler, La Chantrerie  
Nantes, 44307, France  
GIP Arronax, 1 rue Aronnax, Saint-Herblain, 44817, France*

Published 25 February 2014

A dedicated program has been launched on production of innovative radionuclides for PET imaging and for  $\beta$ - and  $\alpha$  targeted radiotherapy using proton or  $\alpha$  particles at the ARRONAX cyclotron. Since the accelerator is also able to deliver deuteron beams up to 35 MeV, we have reconsidered the possibility of using them to produce medical isotopes. Two isotopes dedicated to targeted therapy have been considered:  $^{226}\text{Th}$ , a decay product of  $^{230}\text{Pa}$ , and  $^{186}\text{Re}$ . The production cross sections of  $^{230}\text{Pa}$  and  $^{186}\text{Re}$ , as well as those of the contaminants created during the irradiation, have been determined by the stacked-foil technique using deuteron beams. Experimental values have been quantified using a referenced cross section. The measured cross sections have been used to determine expected production yields and compared with the calculated values obtained using the Talys code with default parameters.

*Keywords:* Production cross section; stacked-foil technique; Talys code; targeted radionuclide therapy; ARRONAX cyclotron.

### 1. Introduction

Targeted radionuclide therapy<sup>1</sup> is one modality to treat cancer that consists of binding a radioactive isotope to a vector in order to target and then destroy tumor cells. The choice of the isotope to be used depends on the characteristics of the targeted tumor:  $\alpha$  emitters will be well suited for isolated and small clusters of carcinogenic

This is an Open Access article published by World Scientific Publishing Company. It is distributed under the terms of the Creative Commons Attribution 3.0 (CC-BY) License. Further distribution of this work is permitted, provided the original work is properly cited.

cells, whereas  $\beta$ - emitters will be used for millimetric tumors. Many isotopes are considered for such applications. Among these are  $^{226}\text{Th}$  and  $^{186}\text{Re}$ , which can be advantageously produced using deuteron beams.  $^{226}\text{Th}$  ( $T_{1/2} = 31$  min) is an  $\alpha$  emitter that has been found to have a greater potential for leukemia therapies<sup>2</sup> than  $^{213}\text{Bi}$ . Indeed, the  $^{226}\text{Th}$  decay produces a cascade of four  $\alpha$  particles with a cumulative energy of 27.7 MeV. Of additional interest is the possibility of using the radionuclide generator system  $^{230}\text{U}/^{226}\text{Th}$ .  $^{230}\text{U}$  ( $T_{1/2} = 21$  days) can be produced directly via  $^{231}\text{Pa}(p,2n)^{230}\text{U}$  and indirectly via  $^{230}\text{Pa}$  ( $T_{1/2} = 17.4$  days) with proton or deuteron beams through  $^{232}\text{Th}(p,3n)^{230}\text{Pa} \rightarrow ^{230}\text{U}$  or  $^{232}\text{Th}(d,4n)^{230}\text{Pa} \rightarrow ^{230}\text{U}$ .

Twelve data sets have been published for the production cross section of  $^{230}\text{Pa}$  using protons<sup>3</sup> but only one using deuterons.<sup>4</sup> A new set of data has been obtained in this study. Production yields have been determined and are compared with those of other production routes in order to determine the best one for  $^{230}\text{U}$  production.  $^{186}\text{Re}$  ( $T_{1/2} = 3.7$  days) is a  $\beta$ - emitter that has been used in clinical trials for palliation of painful bone metastases resulting from prostate and breast cancer.<sup>5</sup> Several cross section measurements have been made since 1966 using proton and deuteron beams on tungsten targets.<sup>3</sup> Previous data show that using deuterons is advantageous compared to protons since the deuteron cross sections are five times higher. As there are some disagreements between the existing data, this study aims to get additional data to better constrain the experimental trend. In both cases, our new data determined via the stacked-foil technique<sup>6</sup> are compared with the existing experimental data and with Talys<sup>7</sup> code calculations performed using default parameters.

## 2. Set-up and Data Measurements

Several stacks of natural tungsten and thorium have been irradiated at the ARRONAX cyclotron<sup>8</sup> in the AX hall devoted to experiments in physics, radiolysis and radiobiology. The stacks were placed in air on an irradiation station called Nice-III. The beam line was sealed using a kapton foil (75  $\mu\text{m}$ ), and the stack was located about 7 cm downstream. Taking into account the 16 MeV threshold for  $^{230}\text{Pa}$ , two beam energies at 30 and 22 MeV were used for the  $^{230}\text{Pa}$  experiments. For the determination of the  $^{186}\text{Re}$  cross section, for which the energy threshold is low (3.6 MeV), deuteron beams at 16.4 MeV were used. One high energy data point, around 22 MeV, was obtained by putting a tungsten foil at the end of one thorium stack irradiated at 30 MeV. All foils were purchased from Goodfellow<sup>®</sup> (France) with high purity ( $\geq 99.6\%$ ). Each thin foil was weighed before irradiation using an accurate scale ( $\pm 10^{-5}\text{g}$ ) and scanned to precisely determine the area. From these values, the thickness has been deduced: around 10  $\mu\text{m}$  for W and Ti and around 45  $\mu\text{m}$  for Th. Titanium monitor foils were placed behind each target foil to record the particle flux along the stack through the  $^{nat}\text{Ti}(d,x)^{48}\text{V}$  reaction, as suggested by IAEA.<sup>9</sup> In each foil, the  $^{48}\text{V}$  activity value was determined after the complete decay of  $^{48}\text{Sc}$  ( $T_{1/2} = 43.67$  h). Nuclear decay data<sup>3</sup> associated with

Table 1. Vanadium-48 half-life and main  $\gamma$  rays.

Radioisotope	$T_{1/2}$ (days)	$E_\gamma$ (keV)	$I_\gamma$ (%)
$^{48}\text{V}$	15.9735 (25)	944.104	7.870 (7)
		983.517	99.98 (4)
		1312.096	98.2 (3)

$^{48}\text{V}$  are summarized in Table 1. In addition to monitor foils, a Faraday cup was placed after the stack to collect the charge and control the intensity during the irradiation. The incident beam energy was fixed by the operating parameters of the cyclotron. The energy through each thin foil was determined in the middle of the foil using the SRIM software.<sup>10</sup> Energy losses in the kapton foil and air were taken into account. Typical irradiations were carried out with about 100 nA during 30 minutes. Each target foil was separated from the stack and, after some cooling time, counting measurements were performed using a high purity germanium detector from Canberra (France) with a low-background lead shield. Gamma spectra were recorded in a suitable geometry previously calibrated with standard  $^{57,60}\text{Co}$  and  $^{152}\text{Eu}$   $\gamma$  sources. The activity values of the radionuclides produced were derived from the spectra and the nuclear decay data<sup>11</sup> given in Table 2, using the Fitzpeak spectroscopy software.<sup>12</sup> The dead time during the countings was always kept below 10% in order to reduce the effect of sum peaks.

Table 2. Properties of radioisotopes produced from natural thorium and tungsten targets.

Radioisotope	$T_{1/2}$ (days)	$E_\gamma$ (keV)	$I_\gamma$ (%)	Contributing reactions	$E_{threshold}$ (MeV)
$^{230}\text{Pa}$	17.4 (5)	951.95	29.1 (14)	$^{232}\text{Th}(d,4n)$	16.013
$^{232}\text{Pa}$	1.31 (2)	969.315	41.6 (19)	$^{232}\text{Th}(d,2n)$	3.537
$^{233}\text{Pa}$	26.967 (2)	312.17	38.6 (4)	$^{232}\text{Th}(d,n) + (d,p)$ decay	0.000
				$^{232}\text{Th}(d,p)$ decay	0.000
$^{186}\text{Re}$	3.7183 (11)	137.157	9.42 (6)	$^{186}\text{W}(d,2n)$	3.626
$^{183}\text{Re}$	70.0 (11)	162.3219	23.3 (4)	$^{182}\text{W}(d,n)$	0.000
		208.8057	2.95 (5)	$^{183}\text{W}(d,2n)$	3.602
		292.7238	3.05 (16)	$^{184}\text{W}(d,3n)$	11.095
				$^{186}\text{W}(d,5n)$	24.180

Production cross section values can be determined from the activation formula in Eq. (1) using the appropriate projectile flux.

$$\sigma = \chi \cdot \frac{Act \cdot A}{\Phi \cdot N_a \cdot \rho \cdot e_f (1 - e^{-\lambda t})} \quad (1)$$

In this equation, the production cross section  $\sigma$  of a radioisotope depends on its measured activity ( $Act$ ), its decay constant ( $\lambda$ ), the target thickness ( $e_f$ ), its atomic number ( $A$ ), its density ( $\rho$ ), its purity ( $\chi$ ), the irradiation duration ( $t$ ) and the projectile flux ( $\Phi$ ). In our experiment, each target foil received the same projectile flux as the monitor foil behind it. It is then easier to use the relative cross section

in Eq. (2) where the knowledge of the projectile flux is no longer necessary. In this equation, the prime parameters are associated with the  $^{48}\text{V}$  monitor while the others relate to the Pa or Re isotopes, depending on the experiment.

$$\sigma = \sigma' \cdot \frac{\chi \cdot \text{Act} \cdot A \cdot \rho' \cdot e'_f (1 - e^{-\lambda't})}{\chi' \cdot \text{Act}' \cdot A' \cdot \rho \cdot e_f (1 - e^{-\lambda t})} \quad (2)$$

To determine the activity associated with each radionuclide of interest, all the target and monitor foils were counted twice with an interval of 2 weeks for more than 24 hours. The cross section uncertainty is estimated with a propagation error calculation. Since all the parameters of Eq. (2) are independent, the total error is expressed as a quadratic sum (Eq. (3)). The main error sources come from the recommended cross section  $\sigma'$  (around 12%),<sup>9</sup>  $^{230,232,233}\text{Pa}$  and  $^{186,183}\text{Re}$  activities (up to 12%),  $^{48}\text{V}$  activity (less than 2%) and thickness uncertainty (around 1%). The contribution of the irradiation time uncertainty is not significant and has been neglected.

$$\frac{\Delta\sigma}{\sigma} = \sqrt{\left(\frac{\Delta\sigma'}{\sigma'}\right)^2 + \left(\frac{\Delta\text{Act}}{\text{Act}}\right)^2 + \left(\frac{\Delta\text{Act}'}{\text{Act}'}\right)^2 + \left(\frac{\Delta e}{e}\right)^2 + \left(\frac{\Delta e'}{e'}\right)^2} \quad (3)$$

### 3. Results

#### 3.1. Production of protactinium radionuclides

The irradiation of a thorium foil by a deuteron beam produces many residues through nuclear and fission reactions. As the specific activity of the final product is directly related to the isotopes of the element of interest, we have optimized our experiment to be able to measure them accurately. For that purpose, the first gamma spectra was acquired 2 days after the end of bombardment to get  $^{232}\text{Pa}$ , which has a half-life of only 1.3 days. In this paper, we only present data for  $^{230,232,233}\text{Pa}$  (all the nuclear parameters used are summarized in Table 2), but data on fission residues have also been collected.

##### 3.1.1. Production of $^{230}\text{Pa}$

We used the 951 keV  $\gamma$  line in the measured spectrum to determine the  $^{230}\text{Pa}$  activity value. Several other  $^{230}\text{Pa}$   $\gamma$  lines have been identified between 397 and 1027 keV with branching ratios higher than 1%. Results from these lines were consistent, giving us confidence in our results. Using the second counting, we verified that the line used was not fed by the decay of another isotope or a fission fragment product and that the measured activity was consistent with the first measurement. The  $^{230}\text{Pa}$  cross section as a function of deuteron energy is plotted in Fig. 1. Our data points are plotted as solid circles whereas the data from J. Rama Rao *et al.*<sup>4</sup> are plotted as empty triangles. The Talys calculated values, generated using default parameters, are plotted as a solid line. Our new data set is consistent with the energy threshold associated with  $^{232}\text{Th}(d,4n)^{230}\text{Pa}$  and shows a maximum of 296

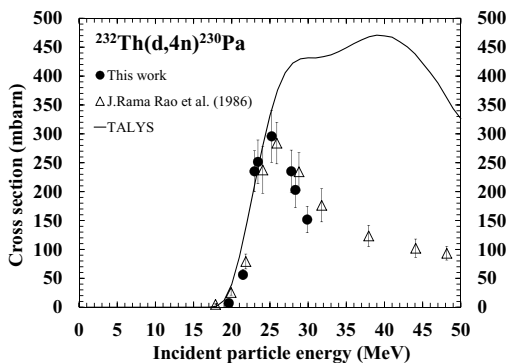


Fig. 1. Production cross section of  $^{232}\text{Th}(d,4n)^{230}\text{Pa}$ .

mbarn at 25.2 MeV. The shape of our data and the maximum value of the cross section are in good agreement with the existing data from Ref. 4. The Talys code calculation shows that neither the shape nor the maximum value of the cross section is reproduced. The  $\gamma$  spectra show that a lot of residues are produced from fission. Since Talys is also able to calculate their contribution, a comparison including all our data is underway.

### 3.1.2. Production of $^{232}\text{Pa}$

$^{232}\text{Pa}$  ( $T_{1/2} = 1.31$  d) emits many detectable  $\gamma$  lines. In their work, J. Rama Rao *et al.*<sup>4</sup> chose to use the 894 keV  $\gamma$  line (22%). In our case, looking at the second counting taken after  $^{232}\text{Pa}$  had totally disappeared, a peak at this energy is still present. We found that this is coming from a sum peak between Pb X-rays (75 keV) from our shielding and the  $^{136}\text{Cs}$   $\gamma$  line (819 keV), a fission fragment produced during the irradiation. We have preferred to use the 969 keV  $\gamma$  line with a higher branching ratio of 42.3% (Table 2), subtracting the contribution of  $^{228}\text{Ac}$  ( $E = 969$  keV,  $I = 15.8\%$ ). Recently, we have performed a new experiment, adding 3 mm of copper shield to attenuate the 75 keV RX emission from lead by a factor of 11. In this experiment, there is no longer the peak in the second measurement, indicating that the source was the one identified. The  $^{232}\text{Pa}$  cross section data are presented in Fig. 2. Due to the  $^{230}\text{Pa}$  energy range of interest, we only measured cross sections in the tail of the curve. The trend is consistent with the existing data set from Ref. 4. Our values are slightly higher, mainly due to the different  $\gamma$  line used and the updated nuclear decay data. In fact, since 1986, the 894 keV  $\gamma$  line branching ratio used by Ref. 4 decreased from 22%<sup>4</sup> to 19.8%.<sup>11</sup> Talys results using default parameters are not in agreement with the data even though the shape is not too bad.

### 3.1.3. Cumulative production of $^{233}\text{Pa}$

$^{233}\text{Pa}$  is produced directly through  $^{232}\text{Th}(d,n)$  but also indirectly by the decay of  $^{233}\text{Th}$  produced via  $^{232}\text{Th}(d,p)$ . Since  $^{233}\text{Th}$  has a short half life ( $T_{1/2} = 21$  min), we were only able to measure the  $^{233}\text{Pa}$  cumulative cross section. These values are plotted and compared to Ref. 4 and Talys in Fig. 2. We used the 312 keV  $\gamma$  line to follow the decay of  $^{233}\text{Pa}$  ( $T_{1/2} = 26.967$  d). Its high branching ratio (Table 2) leads to a small uncertainty associated with the activity value (around 2.7%). Our data are very similar to those of Ref. 4. The small difference can be accounted for by the branching ratio they used ( $I = 37\%$ ), which is lower than the current recommended value ( $I = 38.6\%$ ) listed in the databases.<sup>3,11</sup> The Talys results underestimate the amplitude and the peak width is poorly reproduced.

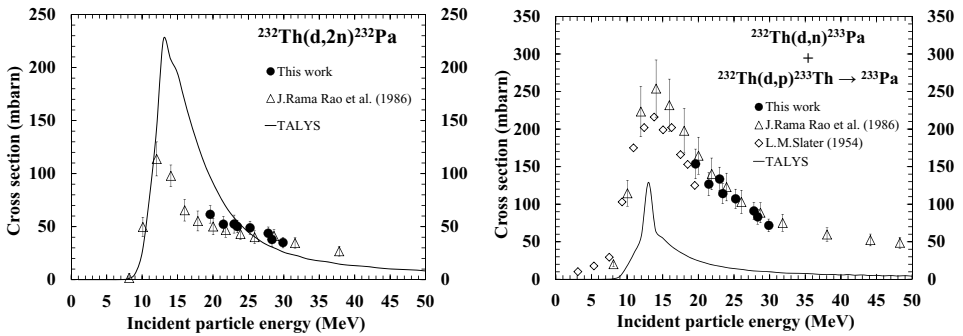


Fig. 2. Production cross section of  $^{232}\text{Th}(d,n)^{233}\text{Pa}$  (on the left) and cumulative production cross section of  $^{233}\text{Pa}$  (on the right).

## 3.2. Production of rhenium radionuclides

In this second part, we have focused on the  $^{186}\text{Re}$  production cross sections induced by deuterons on a natural tungsten target. All of the contaminants produced during this experiment have been measured.  $^{183}\text{Re}$  production cross sections are also presented here. Indeed, due to its long half life ( $T_{1/2} = 70$  d),  $^{183}\text{Re}$  strongly affects the specific activity of the final product.

### 3.2.1. Production of $^{186}\text{Re}$

The  $^{186}\text{Re}$  radionuclide has a half-life of  $T_{1/2}=3.7183$  days and decays 92.53% by  $\beta^-$  emission to  $^{186}\text{Os}$  (stable) and 7.47% by electron capture (EC) to  $^{186}\text{W}$  (stable). Its gamma line,  $E_\gamma=137.157$  keV ( $I = 9.47\%$ ) coming from the  $\beta^-$  decay, is used to measure the activity. In *natW*,  $^{186}\text{Re}$  can only come from the  $^{186}\text{W}$ , the second most abundant isotope (28.6%). Our new data set is presented in Fig. 3 as full circles. These results are very close to the Ref. 13 series in the 7 to 12 MeV range and follow the trend of Ref. 14 up to 17 MeV. Only Ref. 14 and Ref. 15 have data measured with higher beam energies, and our result at 22 MeV is in agreement with their

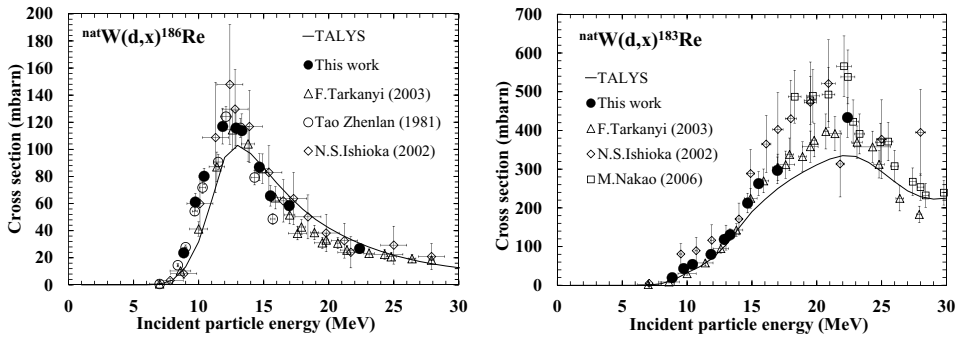


Fig. 3. Production cross section of  $^{nat}\text{W}(d,x)^{186}\text{Re}$  (left) and  $^{nat}\text{W}(d,x)^{183}\text{Re}$  (right).

values. In this case, the Talys code gives satisfactory results, even if the shape is slightly smaller below 12 MeV.

### 3.2.2. Production of $^{183}\text{Re}$

The decay of the  $^{183}\text{Re}$  contaminant was measured using the three main gamma radiations listed in Table 2. It can be produced by four of the tungsten isotopes constituting the natural target. Our results are plotted in Fig. 3 with three other data sets. These data show that the maximum cross section is around 20 MeV but with a different magnitude depending on the data set. Our new values are coherent with the trend of Ref. 14 up to 17 MeV and around 22 MeV. New results above 17 MeV are needed to better discriminate between the different data sets previously published. Talys gives good results below 15 MeV and above 25 MeV. Between these two energies, the different experiments give values 16% to 35% higher than Talys.

## 4. Conclusion

In this work, new data sets for production cross sections induced by deuterons have been obtained. Presented values are in good agreement with the few existing data sets. For thorium, small differences were identified as coming from the recommended nuclear data change. Regarding the production of  $^{230}\text{Pa}$ , we have been able to calculate the  $^{230}\text{U}$  thick target yield (TTY). This value has been compared with the other direct and indirect production routes<sup>17</sup> as shown in Fig. 4.

The TTY of the indirect production routes corresponds to the maximum activity of  $^{230}\text{U}$  reached 27 days after the end of irradiation via  $^{230}\text{Pa}$   $\beta$ -decay and corresponds to  $\approx 2.6\%$  of the  $^{230}\text{Pa}$  activity initially produced. Whatever the production route, direct or indirect, proton beams always give higher  $^{230}\text{U}$  production values than deuteron beams. Both routes using protons are in the same order of magnitude. On one hand, a  $^{232}\text{Th}$  target is easier to obtain and handle than  $^{231}\text{Pa}$ . On the other hand, by using a  $^{232}\text{Th}$  target,  $^{230}\text{U}$  is indirectly produced via the



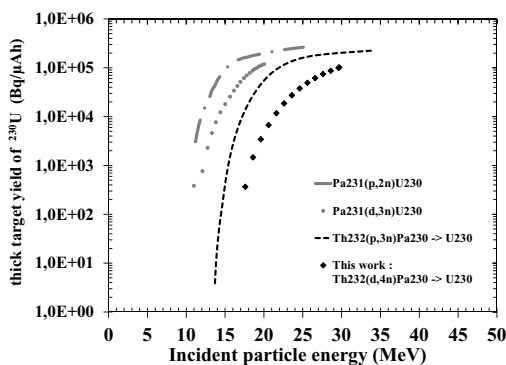


Fig. 4.  $^{230}\text{U}$  thick target yield through different production routes.

$^{230}\text{Pa}$  decay. This means that the  $^{230}\text{U}$  activity is obtained by eluting a  $^{230}\text{Pa}/^{230}\text{U}$  generator.

In the case of  $^{186}\text{Re}$ , the production cross section shows a maximum of 120 mbarn around 12 MeV. Using protons, the maximum value is 23.3 mbarn at 9 MeV (Ref. 9). The deuteron production route is clearly the best choice. All the contaminants created during irradiation were measured since a good optimization process is supposed to find the best compromise between production yield and purity of the final product.

Comparisons with the Talys code have been performed using the default parameters. Differences have been found in the case of a  $^{232}\text{Th}$  target. The fission products will be quantified in our experiments in order to better constrain the code calculation.

## Acknowledgments

The ARRONAX cyclotron is a project promoted by the Regional Council of Pays de la Loire financed by local authorities, the French government and the European Union. This work has been supported in part by a grant from the French National Agency for Research called “Investissements d’Avenir”, Equipex Arronax-Plus n°ANR-11-EQPX-0004.

## References

1. A. Morgenstern et al., *Appl. Radiat. Isot.* **66**, 1275 (2008).
2. C. Friesen et al., *Haematologica*, **94** (suppl.2), 329 (2009).
3. National Nuclear Data Center, BNL (USA), NuDat2 database.
4. J. Rama Rao et al., *Nucl. Phys. A* **448**, 365 (1986).
5. H. Palmedo, J. K. Rockstroh et al., *Radiology* **221**, 256, (2001).
6. S. M. Qaim, *Appl. Radiat. Isot.* **46**(9), 955 (1995).
7. A. J. Koning and D. Rochman, *Nucl. Data Sheets* **113**, 2841 (2012).
8. F. Haddad et al., *Eur. J. Med. Mol. Imaging* **35**, 1377 (2008).

9. IAEA 2007, Charged-particle cross section database for medical radioisotope production, update May 2013.
10. J. F. Ziegler, M. D. Ziegler, J. P. Biersack, *Nucl. Instr. Meth. B* **268**, 1818 (2010).
11. L. F. Ekstrom and R. B. Firestone, *Table of Radioactive Isotopes* version 2.1 (2004).
12. FitzPeaks Gamma Analysis and Calibration Software version 3.66.
13. Tao Zhenlan *et al.*, *Chinese J. of Nuclear Physics* **Vol. 3, Issue 3**, 242 (1981).
14. F. Tarkanyi *et al.*, *Nucl. Instr. Meth. Phys. Res. B* **211**, 319 (2003).
15. N. S. Ishioka *et al.*, *J. Nucl. Science and Tech. Supply* **Vol. 2** 1334 (2002).
16. M. Nakao *et al.*, *Nucl. Instr. Meth. Phys. Res. A* **562** 785 (2006).
17. A. Morgenstern *et al.*, *Physical Review C* **80**, 054612 (2009).